

# Absorption Properties of Alkoxy-Substituted Thienylene–Vinylene Oligomers as a Function of the Doping Level

E. E. Havinga\*,† and C. M. J. Mutsaers

*Philips Research Laboratories, Prof. Holstlaan 4, 5656 AA Eindhoven, The Netherlands*

L. W. Jenneskens

*Debye Institute, Department of Physical Organic Chemistry, Utrecht University, Padualaan 8, 3584 CH Utrecht, The Netherlands*

*Received September 29, 1995. Revised Manuscript Received December 12, 1995*<sup>⊗</sup>

In an attempt to improve on the properties of PEDOT (poly(3,4-ethylenedioxythiophene)) as a stable, conducting, and transparent coating we synthesized four different alkoxy-substituted poly(thienylene–vinylene)s, **1–4**, using the Stille coupling reaction. The oligomers and polymers obtained were characterized and their NIR–vis absorption spectra were measured as a function of doping, both electrochemically as films and chemically in solution. Similar spectra of PEDOT films were gathered for comparison. In PEDOT a change in doping level does not change the energies of the absorption bands, while for the other polymers the bands shift markedly and the NIR peak at high doping level lies at a higher energy. The polymers **1–4** are much less suited for the intended coatings than PEDOT. Possible reasons for this are discussed.

## 1. Introduction

Conductive transparent coatings are a promising potential field of application for doped through-conjugated polymers. Coatings on cathode-ray tubes to prevent static charging or to provide electric shielding as well as transparent electrodes in liquid-crystalline displays or polymeric light-emitting diodes are just a few examples. Nowadays, inorganic materials like doped stannates (e.g., antimony–tin oxide) or doped indates (e.g., indium–tin oxide (ITO)) are used since they combine a high transmittance of visible light (90%) with a low electrical resistivity ( $10\text{--}20\ \Omega\ \text{square}^{-1}$ ). However, their brittle character as well as the complicated high-temperature processing involved make them less attractive. Solvent processible doped through-conjugated polymers may be an alternative, because of simple processing techniques such as spin-coating, dip-coating, inkjet printing, and silk-screen printing.

Poly(3,4-ethylenedioxythiophene) (PEDOT) possesses a relatively low optical absorption coefficient ( $7.1 \times 10^3\ \text{cm}^{-1}$  at 2.1 eV) combined with high conductivity ( $200\ \text{S cm}^{-1}$ ).<sup>1–3</sup> Very thin films of about 500 Å fulfill the optical requirements of an ES-coating on cathode-ray tubes, viz., a transmittance of 80–90% between 380 and 780 nm. However, the electric requirements ( $1000\ \Omega\ \text{square}^{-1}$ ) are only barely met. The specific conductivity of PEDOT is already very high for doped through-conjugated polymers. Only for well oriented polymers

have higher conductivities been reported. Therefore, potential improvements have to be explored in the optical rather than in the electrical properties. Moreover, PEDOT is insoluble and its processing is not easy.<sup>4</sup> Solubility might be improved by replacing the ethylene dioxide side group by alkoxy side chains or adding an alkyl group to the ethylenic carbon.

In this paper we report on chemical modifications of PEDOT, intended to improve the transparency and solubility with preservation of the high conductivity. The polymers prepared (see Figure 1) are poly(3,4-(octylenedioxy-1,2)-thiophene) (PEDOT-C<sub>8</sub>) and four alkoxy-substituted poly(thienylene–vinylene)s (PAOTVs) **1–4**, synthesized using the Stille coupling reaction.<sup>5</sup> The vinylene spacer between the alkoxy-substituted thiophene repeat units was introduced to decrease the steric hindrance which is known to occur in alkoxy-substituted thiophenes.<sup>6</sup> Steric hindrance leads to a less planar conjugated system, having a larger bandgap. Upon doping the broad (bi)polaron absorption band(s) would shift toward the visible region, which might spoil the contemplated transparency. The optical absorption spectra of these polymers were measured and are compared with those of PEDOT and of polythiophene. Although most of the new polymers are an improvement on PEDOT as to solubility, their transparency and especially the conductivity is much lower. A striking correlation between the change of the optical spectra upon doping and the final conductivity at maximum dope is found.

† Also at Laboratory of Technical Organic Chemistry, Technical University of Eindhoven, The Netherlands.

<sup>⊗</sup> Abstract published in *Advance ACS Abstracts*, February 1, 1996.

(1) Heywang, G.; Jonas, F. *Adv. Mater.* **1992**, *4*, 116–118.

(2) Pei, Q.; Zuccarello, G.; Ahlskog, M.; Inganäs, O. *Polymer* **1994**, *35*, 1347–1351.

(3) Gustafsson, J. C.; Liedberg, B.; Inganäs, O. *Solid State Ionics* **1994**, *69*, 145–152.

(4) de Leeuw, D. M.; Kraakman, P. A.; Bongaerts, P. F. G.; Mutsaers, C. M. J.; Klaassen, D. B. M. *Synth. Met.* **1994**, *66*, 263–273.

(5) Stille, J. K. *Angew. Chem., Int. Ed. Engl.* **1986**, *25*, 508–524.

(6) Havinga, E. E.; Rotte, I.; Meijer, E. W.; ten Hoeve, W.; Wynberg, H. *Synth. Met.* **1991**, *41–43*, 473–478.

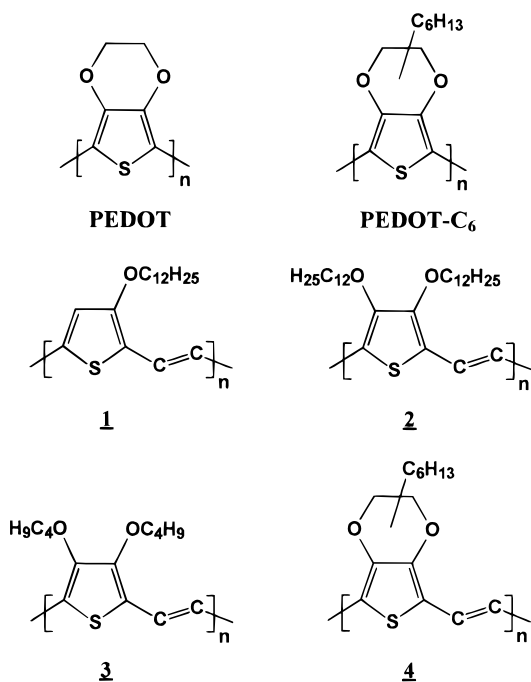


Figure 1. Polyalkoxythiophenes and PAOTVs.

## 2. Experimental Section

**2.1. Materials.** The starting materials lithium acetylide ethylenediamine complex (90%), tributyltin chloride (96%), tributyltin hydride (97%), *n*-butyllithium (1.6 mol/L in hexane), and tetrakis(triphenylphosphine) palladium(0) (99%, Aldrich) were used without further purification. The radical initiator 2,2-azobis(methylpropionitrile) (AIBN) as well as the organic solvents (p.a.) were purchased from Merck and used as received. 3,4-Ethylenedioxythiophene (EDOT, Bayer) was distilled before use (64 °C at  $6 \times 10^{-5}$  bar, colorless liquid,  $n_D = 1.5732$  at 25 °C,  $^1\text{H NMR}$  ( $\text{CDCl}_3$ )  $\delta = 4.18$  (s, 4 H), 6.35 (s, 2 H)). The monomers 3-(dodecyloxy)thiophene (mp 26.7–29.8 °C), 3,4-bis(dodecyloxy)thiophene (mp 45.7–48.4 °C), 3,4-dibutoxythiophene and 3,4-(octylenedioxy-1,2)thiophene were obtained from Syncom B.V. (Groningen, The Netherlands). 3,4-(Octylenedioxy-1,2)thiophene was distilled before use (90–120 °C at  $5.5 \times 10^{-5}$  bar, yellow liquid,  $n_D = 1.5136$  at 25 °C,  $^1\text{H NMR}$  ( $\text{CDCl}_3$ )  $\delta = 0.9$  (t, 3 H), 1.3 (m, 6 H), 1.55 ppm (2 H), 1.68 (m, 2 H), 3.84 (m, 1H), 4.1 (m, 2 H), 6.3 (s, 2 H)). 3,4-Dibutoxythiophene was distilled before use (118–120 °C at 0.1 mbar, light yellow liquid,  $n_D = 1.4995$  at 25 °C,  $^1\text{H NMR}$  ( $\text{CDCl}_3$ )  $\delta = 0.97$  (t, 6 H), 1.48 (m, 4 H), 1.77 (m, 4 H), 3.95 (t, 4 H), 6.15 (s, 2 H)). *p*-Toluenesulfonic acid (99%), methanesulfonic acid (99%), iron(III) nitrate nonahydrate (p.a.) and 2,3-dicyano-4,5-dichloro-1,4-benzoquinone (98%) were purchased from Janssen Chimica and used without further purification.

**2.2. Equipment.** Refractive indexes were measured at 25 °C using a Carl Zeiss refractometer. Melting points were determined using a microscope and a hot stage (Mettler FP52) which was linked to a temperature controller (Mettler FP5). The  $^1\text{H NMR}$  spectra at 300 MHz in deuterated chloroform (Merck) were recorded on a Bruker MSL300 spectrometer. Chemical shifts are reported in  $\delta$  units relative to tetramethylsilane. The molecular weight distributions were determined using Gel Permeation Chromatography (GPC). The copolymers were dissolved ( $\approx 0.1$  mg in 1 mL tetrahydrofuran (Merck, Lichrosolve)) and filtered before use (0.5  $\mu\text{m}$ , Millipore Millex LCR). Two columns in series (PLgel-5- $\mu\text{m}$ -MIXED-C) with a linear molecular weight range between  $2 \times 10^2$  and  $3 \times 10^6$  were used. Polystyrene (PL-Easical) was used as calibration standard (10 molecular weights ranging from 580 to  $8.5 \times 10^6$ ). Tetrahydrofuran (Merck, Lichrosolve) was used as eluent. The stabiliser of tetrahydrofuran (butylated hydroxytoluene, MW 220) was also used as calibration point. The UV detection was performed at the absorption maximum of the oligomer in question. The elements C, H, O, and S were determined using a Carlo Erba EA 1106, an elemental

analyzer based on flash combustion of the sample. The combustion products were separated by gas chromatography using a thermal conductivity detector. Br and Cl were determined by ion chromatography using a Dionex 2010i equipped with a AG4/AS4 column. A solution of 0.75 mM  $\text{NaHCO}_3/2.0$  mM  $\text{Na}_2\text{CO}_3$  was used as eluent. Pd and Sn were determined by mass spectroscopy using a PlasmaQuad II Plus ICP-MS.

The UV-vis-NIR absorption spectra were recorded on a Perkin-Elmer Lambda 9 spectrophotometer (120 nm  $\text{min}^{-1}$ , slit width 1 nm (UV region) or adapted automatically (NIR)). Oscillator strengths,  $f$ , were determined by numerical integration using  $f = 4.32 \times 10^{-9} \int \epsilon \, d\nu$ , where  $\nu$  is the frequency in  $\text{cm}^{-1}$  and  $\epsilon$  the molar extinction coefficient in  $1 \text{ mol}^{-1} \text{ cm}^{-1}$ . The boundaries of the integration were the frequencies at which either  $\epsilon = \epsilon_{\text{max}}/50$  or at which a minimum with a neighboring absorption was found. Absorption peaks near the cutoff boundary of the instrument were extrapolated to zero by hand.

Changes in oscillator strengths were obtained by subtracting between identical boundaries. Polymer solutions of  $10^{-4}$ – $10^{-3}$  mol  $\text{L}^{-1}$  in chloroform (Merck) were doped using a solution of ferric chloride (Aldrich, 98%, anhydrous) in chloroform (Merck). Using a Hamilton microsyringe, portions of 40  $\mu\text{L}$  of the solution of the oxidizing agent ( $\sim 10$  mol %  $\text{FeCl}_3$  with respect to the repeat unit) were added to 2 mL of polymer solution. The spectra were corrected for dilution effects.

The oxidation potentials of films were determined by measuring cyclovoltammograms (CVs) at various scanning speeds of 25–500 mV/s in a homemade cell provided with a reference electrode (saturated calomel electrode, SCE (Radiometer, REF401)), a platinum wire as a counter electrode and a platinum electrode of  $7.85 \times 10^{-3} \text{ cm}^2$  as a work electrode. The half-wave potential,  $E_{\text{ox}}$ , was found as the average value of oxidation and reduction peaks, extrapolated to scanning speed 0 by straight lines through the maxima. A solution of tetrabutylammonium hexafluorophosphate (0.25 M, electrochemical grade, Fluka) in acetonitrile (0.25 M, HPLC grade, Janssen Chimica) was used as the electrolyte solution. The potential was varied using a computer controlled potentiostat (EG&G, 263A). The potentiostat used was also used to determine the accumulated charge during doping, which is a measure of the doping level. Spectroelectrochemical experiments were performed in a specially designed electrochemical cell with the same electrolyte solution and reference electrode and a small narrowly meshed cylindrical platinum net as a counter electrode. Polymer solutions (10 mg in 2 g of chloroform (Aldrich)) were filtered over 0.5  $\mu\text{m}$  (Millipore, Millex-SR) and spin-coated (1000 rpm, 30 s) onto a work electrode consisting of an ITO-coated glass substrate ( $14 \Omega \text{ square}^{-1}$ , area = 1.767  $\text{cm}^2$ ) using a Convac spincoater (ST145/1001 GS). The layers were dried on a hot plate (110 °C, 1 min). The layer thickness ( $\sim 500$  Å) was measured using a surface profile measuring system (Sloan Dektak 3030). The densities of films were determined by weighing, accuracy about 0.02  $\text{g cm}^{-3}$ . Prior to the electrochemical doping procedure, the cell was purged with dry nitrogen (60 min) to remove oxygen from the electrolyte solution. Absorption spectra were measured at various potentials going from the undoped state to the maximum doped state. At each potential change a waiting time of 2 min was exercised. It was verified that after that time no change in absorption spectrum could be observed. After maximum doping was reached, the films were dedoped again to check that no decomposition had occurred during doping. This spectrum is marked with an asterisk. The absorption between 1630 and 1770 nm due to water was removed from the spectrum, and the missing data points were interpolated.

The electrical resistance of films was measured with a homemade standard four-point probe. Films of the PAOTVs were doped in a nitrogen atmosphere saturated with iodine vapor. Doping was also performed by mixing a solution of the PAOTV (10 mg in 1 g of dichloromethane) with a solution of 2,3-dicyano-4,5-dichloro-1,4-benzoquinone (DDQ, 1.5 mg in 0.5 g of dichloromethane) and a drop of methanesulfonic acid. After spin-coating (500 rpm, 3 s and 1000 rpm, 27 s) the

electrical resistance of the film was measured (no bake step was applied after the spin-coating procedure).

**2.3. Synthetical Procedures. Tris(*p*-toluenesulfonate)-iron(III) hexahydrate:** A concentrated ammonia solution (28–30 wt %, 150 mL) was added to a solution of iron(III) nitrate nonahydrate (210 g) in 1.5 L of water. The solid reaction product, ferric hydroxide, was removed by centrifugation and added to a solution of *p*-toluenesulfonic acid monohydrate (230 g) in 600 mL of methanol. The mixture was refluxed for 16 h, and the excess iron(III) hydroxide was separated from the solution by centrifugation. The resulting solution was filtered over 0.2  $\mu\text{m}$ . The solvent was removed at reduced pressure and the resulting solid was dried at reduced pressure at 50 °C for 48 h, yield 619 g (90%). The hygroscopic red solid was exposed to ambient conditions resulting in tris(*p*-toluenesulfonate)iron(III) hexahydrate (yellow), which is highly soluble in 1-butanol.

*Tributylethynyltin* was prepared according to a procedure described in literature.<sup>6</sup> The yield after distillation (96–98 °C at  $8 \times 10^{-5}$  bar) was 30.9%,  $n_D$  1.4750 (25 °C), <sup>1</sup>H NMR (CDCl<sub>3</sub>)  $\delta$  = 0.9 (t, 9 H), 1.02 (t, 6 H), 1.34 (m, 6 H), 1.55 (m, 6 H), 2.2 (s, 1 H).

(*E*)-1,2-Bis(tributyltin)ethylene was prepared according to a literature procedure.<sup>8</sup> Yield after distillation (183–189 °C at  $6 \times 10^{-5}$  bar) was 93.2%,  $n_D$  1.5003 (25 °C), <sup>1</sup>H NMR (CDCl<sub>3</sub>)  $\delta$  = 0.9 (t, t, 30 Hs), 1.3 (m, 12 Hs), 1.5 (m, 12 Hs), 6.9 (s, 2 Hs).

**2,5-Dibromo-3-(or 3,4-di)alkoxythiophenes, general procedure:** A three-necked round-bottom flask of 250 mL equipped with a magnetic stirring bar, a reflux condenser and a nitrogen/vacuum inlet was charged with *N*-bromosuccinimide and 3-(dodecyloxy)thiophene (molar ratio 2:1) in carbon tetrachloride. The flask was evacuated and filled with nitrogen (three times). The reaction mixture was heated to 90 °C and stirred at this temperature for 5 h and then kept overnight at room temperature. After filtration of the solid (succinimide), the solvent was removed under reduced pressure at 50 °C. Purification was performed by column chromatography using silicagel/dichloromethane (silicagel 60 (Merck), particle size 0.040–0.063 mm).

**2,5-Dibromo-3-(dodecyloxy)thiophene:** yield 25.4%, <sup>1</sup>H NMR (CDCl<sub>3</sub>)  $\delta$  = 0.89 (t, 3 H), 1.27 (s, 16 H), 1.44 (m, 2 H), 1.75 (m, 2 H), 4.00 (t, 2 H), 6.78 (s, 1 H).

**2,5-Dibromo-3,4-bis(dodecyloxy)thiophene:** yield 92.3%, melting point: 30.5 °C, <sup>1</sup>H NMR (CDCl<sub>3</sub>)  $\delta$  = 0.88 (t, 3 Hs), 1.25 (s, 32 Hs), 1.44 (m, 2 Hs), 1.72 (m, 2 Hs), 4.04 (t, 2 Hs).

**2,5-Dibromo-3,4-dibutoxythiophene:** yield 64.3%, <sup>1</sup>H NMR (CDCl<sub>3</sub>)  $\delta$  = 0.96 (t, 6 H), 1.49 (m, 4 H), 1.71 (m, 4 H) 4.05 (t, 4 H).

**2,5-Dibromo-3,4-(octylenedioxy-1,2)thiophene:** yield 72.9%, <sup>1</sup>H NMR (CDCl<sub>3</sub>)  $\delta$  = 0.90 (t, 3 H), 1.25–1.80 (m, 10 H), 3.91, 4.23, 4.28 (m, d, d, 2 H), 4.14 (m, 1 H).

**PAOTVs, general procedure:** A three-necked round bottom flask of 250 mL equipped with a magnetic stirring bar, a reflux condenser, and a nitrogen/vacuum inlet was charged with the thiophene derivative dissolved in a mixture of dimethylformamide/tetrahydrofuran. Tetrakis(triphenylphosphine)palladium(0) (5 mol % with respect to the dibromo compound) was dissolved in this solution which resulted in a clear yellow solution. After the addition of (*E*)-1,2-bis(tributyltin)ethylene (equimolar with respect to the dibromo derivative) the system was evacuated and filled with nitrogen (three times). The reaction mixture was heated to 100 °C for 2.5 or 6 h. The mixture was then poured into a mixture of water (5 vol %) in methanol and stirred for 1 h. The resulting black coloured solid was separated by filtration and washed with methanol/water until the filtrate was colorless. The solid was then washed with methanol and dried at 60 °C in vacuum for 1 h.

**Poly(3-(dodecyloxy)thienylene-vinylene) (1):** yield 46.3%,  $\rho$  = 1.17 g cm<sup>-3</sup>,  $E_{ox}$  = +0.36 V vs SCE.

**Poly(3,4-bis(dodecyloxy)thienylene-vinylene) (2):** yield 89.3%,  $\rho$  = 1.28 g cm<sup>-3</sup>,  $E_{ox}$  = +0.65 V vs SCE. The synthesis was repeated with a reaction time of 6 h (2\*), yield 32.2%.

**Poly(3,4-dibutoxythienylene-vinylene) (3):**  $\rho$  = 1.36 g cm<sup>-3</sup>,  $E_{ox}$  = +0.57 V vs SCE, yield 58.2%.

**Table 1. GPC Molecular Weight Distribution**

PAOTV	$M_0^a$	$M_n$	$P_n$	$M_w$	$D$	reaction time (h)
<b>1</b>	292	2400	8	3500	1.5	6
<b>2</b>	476	12000	25	23000	1.9	2.5
<b>2<sup>a</sup></b>	476	24000	50	37000	1.5	6
<b>3</b>	252	4700	19	9400	2.0	6
<b>4</b>	250	1800	7	2800	1.6	2.5
<b>4<sup>a</sup></b>	250	1500	6	1900	1.3	6

<sup>a</sup> Molecular weight repeat unit.

**Poly(3,4-(octylenedioxy-1,2)thienylene-vinylene) (4):**  $\rho$  = 1.24 g cm<sup>-3</sup>, yield 38.3%,  $E_{ox}$  = +0.44 V vs SCE. The reaction was repeated with a reaction time of 6 h (4\*), yield 52.3%.

**Poly(3,4-ethylenedioxythiophene):** A solution consisting of tris(*p*-toluenesulfonate)iron(III) hexahydrate (0.46 g, 0.68 mmol), imidazole (0.020 g, 0.29 mmol), and 1-butanol (1.5 g) was mixed with EDOT (0.05 g, 0.35 mmol). The resulting solution was filtered over 0.5  $\mu\text{m}$  (Millipore, Millex-SR) and spin-coated onto a glass or an ITO-coated glass substrate (3 s, 500 rpm and 7 s, 1000 rpm). Polymerization took place upon heating at 110 °C (1 min on hot plate). The remaining ferro salt was removed by soaking the polymer film in 1-butanol. The film (~500 Å) was dried using compressed air,  $\rho$  = 1.69 g cm<sup>-3</sup>,  $E_{ox}$  = -0.13 V vs SCE. The same procedure was used to prepare films of PEDOT-C<sub>6</sub>, poly(3,4-(octylenedioxy-1,2)-thiophene,  $\rho$  = 1.68 g cm<sup>-3</sup>,  $E_{ox}$  = -0.04 V vs SCE.

**2.4. Characterization.** The synthesized PAOTVs have a low degree of polymerization,  $P_n$  (see Table 1). In fact, only co-oligomers were formed. This is probably due to the instability of the brominated starting compounds. The three oils colored indigo blue with time, even when stored at 5 °C. However, the <sup>1</sup>H NMR spectra of the blue-colored dibromo compounds are the same as the original spectra. Only 2,5-dibromo-3,4-bis(dodecyloxy)thiophene (waxlike solid) was stable at room temperature. Rapid deterioration of the dibromides at the reaction conditions could explain the low degrees of polymerization reached for **1**, **3**, and **4**, and the failure to increase the molar mass by increasing the reaction time (**4\***). The significantly higher degree of polymerization of **2**, increasing with reaction time (**2\***), then, reflects the higher stability of the corresponding dibromide. For the low yield of **2\*** we have, however, no explanation. Destannylation of the reactant during the reaction may also contribute to the low molecular weight. Moreover, the solubility of the PAOTVs decreases as the molecular weight increases. If the growing polymer precipitates the polymerization stops. Since the final reaction mixtures were turbid, this explanation cannot be ruled out. The dispersion,  $D = M_w/M_n$ , is reasonably low. The PAOTVs are soluble in chloroform, dichloromethane, and tetrahydrofuran. In the case of **2\*** the higher molecular weight already limits the solubility. Despite the low degree of polymerization, the synthesized "polymers" are still suitable to investigate the relationship between chemical structure and optical properties. Going from the monomer to the hexamer, the decrease in bandgap is large.<sup>9</sup> Beyond the hexamer, the optical and electric properties of oligomers resemble those of polymers, albeit that the conductivity of a polymer is about one order of magnitude larger.

Elemental analysis showed that the elements C, H, O, and S are in reasonable agreement with the calculated values (Table 2). The latter are based on the measured degree of polymerization and the (disputable) assumption that on average each polymer chain possesses one bromo and one tributyltin end group. The impurities are limited to small amounts of Pd from the catalyst used and some chlorine due to tributyltin chloride that is formed upon the transmetalation.

The <sup>1</sup>H NMR spectra of the synthesized oligomers are in agreement with expectations for the contemplated alkoxy-substituted PTV oligomers. The resonance peaks are very broad due to the polymeric character. The two protons at the vinylene bridge are located at 6.9 ppm. The resonance peaks of the protons of the alkoxy side chains lay between 0.8 and

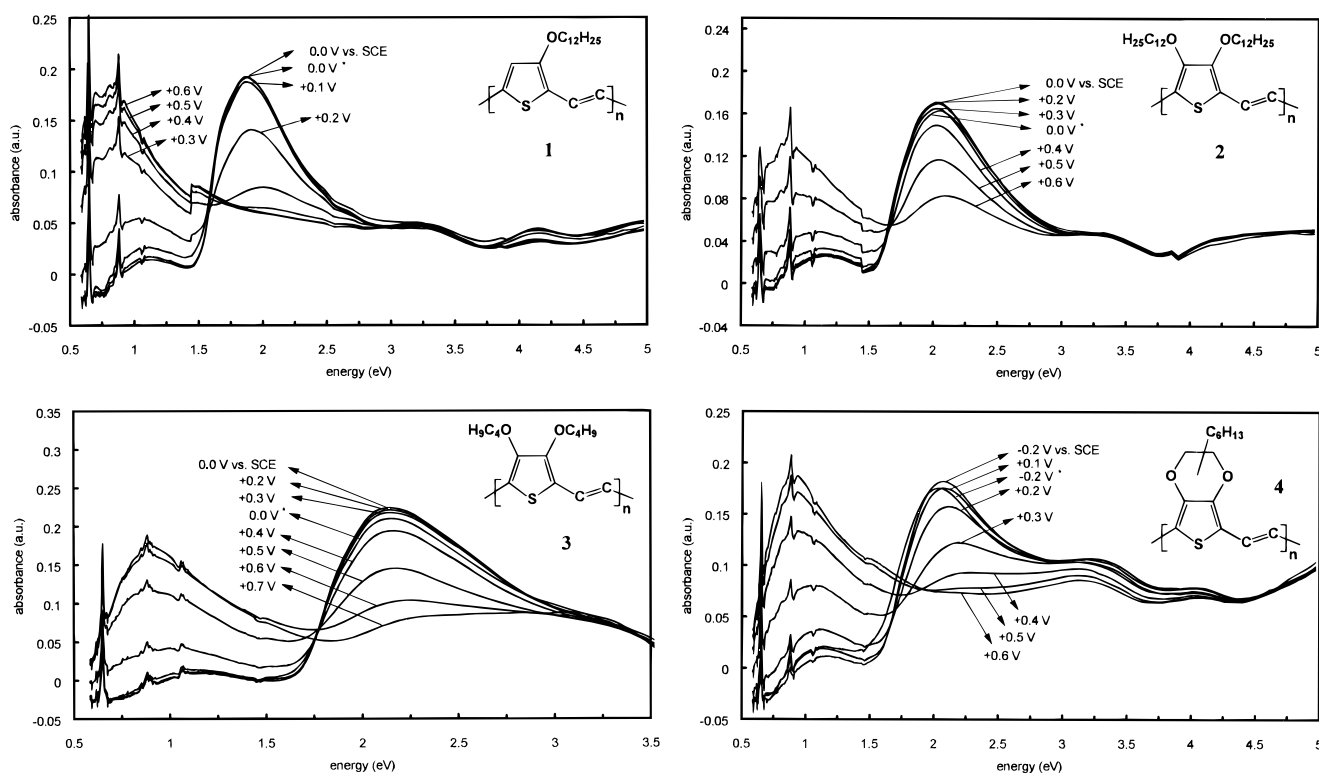


**Figure 2.** Absorption spectra of films of PAOTVs with electrochemical doping.

**Table 2. Elemental Analysis (wt %)<sup>a</sup>**

element	1		2		3		4	
	obs	calc	obs	calc	obs	calc	obs	calc
C	70.7	71.8	74.5	74.1	62.9	64.9	63.1	63.2
H	9.7	9.4	11.1	10.8	7.55	7.9	6.9	7.2
O	4.7	5.1	6.2	6.4	10.8	11.8	10.8	11.0
S	9.8	10.2	7.2	6.4	11.9	11.8	10.6	11.0
Sn	2.4	2.0	0.2	1.3	1.9	2.3	1.0	4.5
Pd	0.8		0.1		0.9		1.1	
Br	0.7	1.4	1.1	0.9	0.7	1.5	3.5	3.1
Cl	0.4		0.6		2.1		2.4	

<sup>a</sup> Relative accuracy C and S 3%, for the rest 5%.

1.8 ppm and at 4.1 ppm (methylene protons next to an oxygen atom).

### 3. Results

**3.1. Poly(alkoxy-substituted thienylene–vinylene)s.** The poly(alkoxy-substituted-thienylene–vinylene)s (PAOTVs) **1–4** are soluble in common organic solvents. Therefore, their absorption spectra were determined both for films doped electrochemically (Figure 2) and for solutions in chloroform and doped by adding increasing amounts of a ferric chloride solution as an oxidant (Figure 3). The overall doping reaction in that case reads<sup>10</sup>



The two absorption bands at 3.43 and 3.86 eV in the solutions are due to the counterion  $\text{FeCl}_4^-$ ;  $\text{FeCl}_3$  gives a single absorption band at 3.65 eV. The features below the band gaps in the solid state spectra of undoped PAOTVs are probably due to charged stacking defects. They are absent in the solution spectra. The bandgaps of undoped PTVs are somewhat lower in the solid state

as compared to the solution experiments (see Table 5 in section 4). The bandgap of **3** is in agreement with the literature,<sup>11</sup> the bandgap of **1** is nearly equal to that of poly(3-ethoxythienylene–vinylene).<sup>12</sup>

The observed changes in the absorption spectra upon doping are very similar in both solid and solution, including a marked shift in the  $\pi-\pi^*$  absorption band toward higher energies. Only the high energy and the large width of the NIR band in **4** in strongly doped solutions are striking exceptions, and at low doping levels in solution one can discern two NIR maxima against only one in the corresponding solid-state spectra. The published spectrum of a  $\text{FeCl}_3$ -doped film of poly(3-ethoxythienylene–vinylene)<sup>12</sup> shows a maximum at about 1.2 eV, a much higher energy than that we find for **1**. The decrease in oscillator strengths of the  $\pi-\pi^*$  absorption bands in the visible in going from undoped samples to maximum doping level is smaller than the increase of the NIR bands (see Table 3). The  $\pi-\pi^*$  absorption bands of the polymers **2** and **3** do not completely disappear at maximum doping level. This is related to incomplete doping, due to the oxidation potential of these polymers (+0.57 and +0.65 V vs SCE, respectively), which is somewhat higher than that of ferric chloride (+0.53 V vs SCE) and around the maximum potential used in the electrochemical doping, viz. 0.6 V vs SCE. Up to this potential the electrochemical doping is reversible, as can be seen from the curves 0.0 V\*, taken after the curve of 0.6 V. At higher potentials all four PTVs start to decompose. The maximum doping levels, both in solution and in films, are about  $0.25 \pm 0.05$  dopants per repeat unit. More accurate determination for the solution experiments are hampered by a rather large uncertainty in the amount

(11) van Dort, P. C.; Pickett, J. E.; Blohm, M. L. *Synth. Met.* **1991**, *41–43*, 2305–2308.

(12) Jen, K.-Y.; Eckhardt, H.; Jow, T. R.; Shacklette, L. W.; Elsenbaumer, R. L. *J. Chem. Soc., Chem. Commun.* **1988**, 215–217.

(10) Pecker, S.; Janossy, A. In *Handbook of Conducting Polymers*; Skotheim, T. A., Ed.; Marcel Dekker: New York, 1986; Vol. 1, p 55.

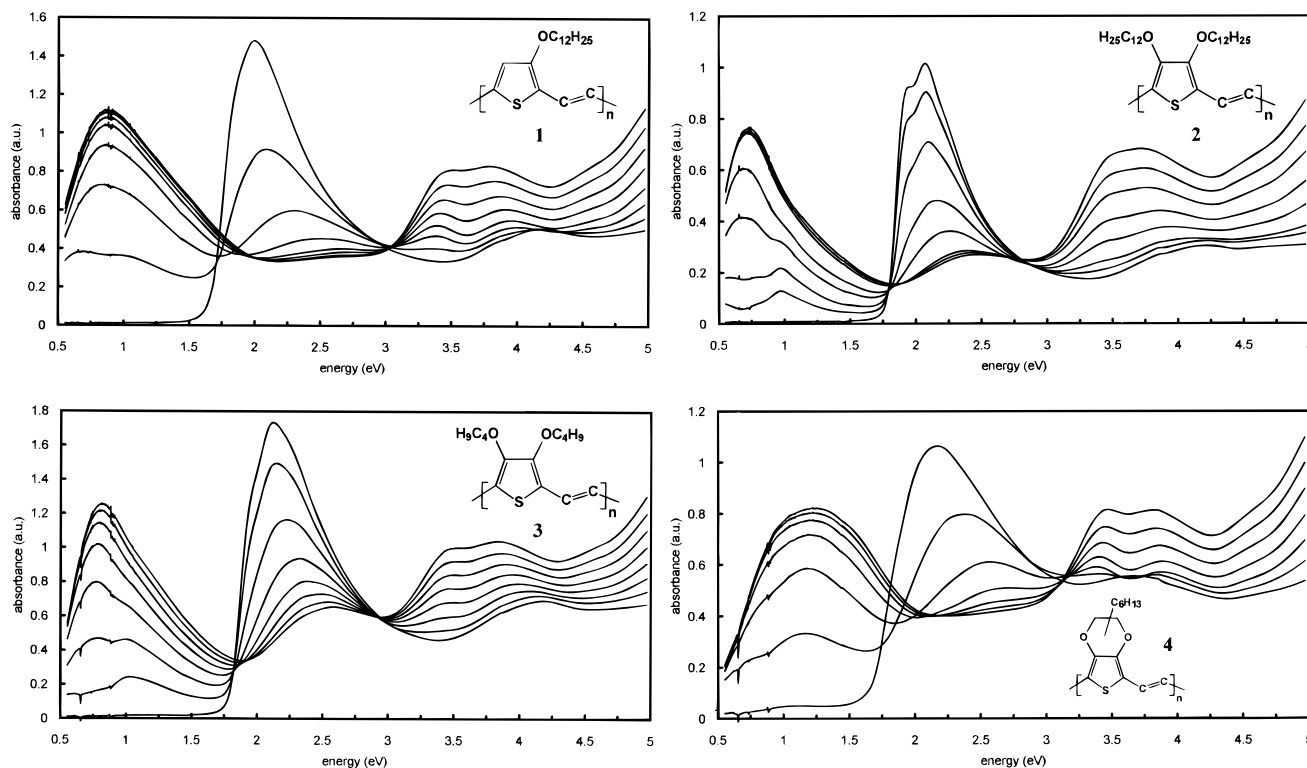


**Figure 3.** Absorption spectra of solutions of PAOTVs in dichloromethane with doping by ferric chloride.

**Table 3. Change of Oscillator Strength per Repeat Unit,  $\Delta f$ , at Maximum Doping**

PAOTV	solid			film		
	$\Delta f(\text{vis})$	$\Delta f(\text{NIR})$	$\Delta(\Delta f)$	$\Delta f(\text{vis})$	$\Delta f(\text{NIR})$	$\Delta(\Delta f)$
<b>1</b>	-0.19	0.27	0.08	-0.14	0.22	0.08
<b>2</b>	-0.23	0.31	0.08	-0.15	0.20	0.05
<b>3</b>	-0.17	0.24	0.07	-0.15	0.17	0.02
<b>4</b>	-0.14	0.21	0.07	-0.10	0.19	0.09

**Table 4. Specific Conductivity,  $\sigma$  (S/cm), of Doped Films**

polymer	$\sigma(\text{I}_3^-)$	$\sigma(\text{DDQ})$	$\sigma(\text{as prep})$
<b>1</b>	2.1	2.0	
<b>2</b>	0.1	0.07	
<b>3</b>	0.002	0.2	
<b>4</b>	0.045	0.35	
PEDOT			400
PEDOT-C <sub>6</sub>			40

of unchanged  $\text{FeCl}_3$  present in the heavily doped samples, estimated from the UV-vis spectra. In the electrochemistry experiments long tails in the currents, due to side reactions, had to be eliminated. Their contribution to the total current were estimated by extrapolation of currents at times after completion of doping toward smaller times.

The specific conductivities of PAOTV films doped with iodine vapor are shown in Table 4. The low oxidation potential of iodine (+0.30 V vs SCE) results in incomplete doping, except perhaps for **1**. Therefore, we also tried to effectuate doping using a stronger oxidant, 2,3-dicyano-5,6-dichlorobenzoquinone/methanesulfonic acid in dichloromethane. Despite the low quality of the resulting samples the conductivities measured were much higher (Table 4) but still orders of magnitude lower than those of PEDOT and of PEDOT-C<sub>6</sub>.

**3.2. Poly(3,4-ethylenedioxythiophene).** Doped poly(3,4-ethylenedioxythiophene), PEDOT, is insoluble in all common solvents we tried. The low oxidation potential of -0.13 V vs SCE implies a high stability in

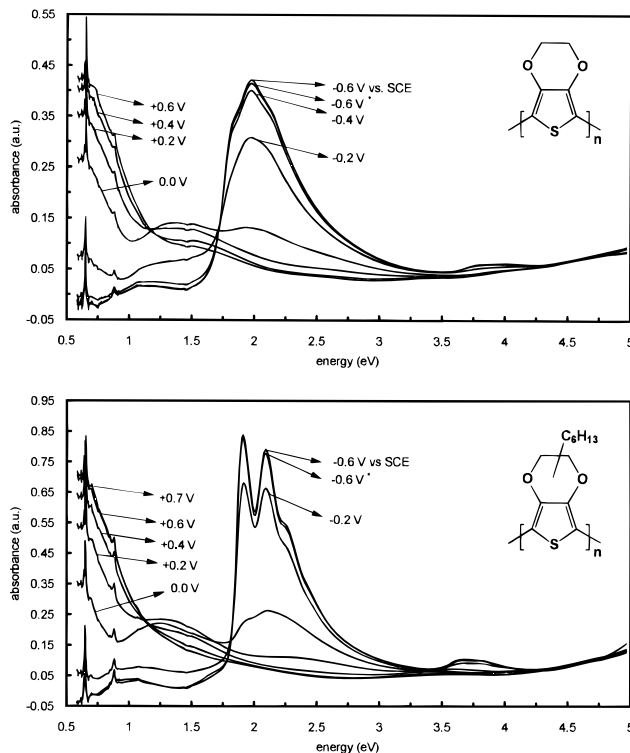


**Figure 4.** Absorption spectra of films of PEDOT and PEDOT-C<sub>6</sub> with electrochemical doping.

the p-type doped state. Coatings of doped PEDOT could be dedoped only in a thin top layer by using a reducing agent, but electrochemically complete dedoping was obtained. The absorption spectra of the PEDOT film at various stages of electrochemical doping are shown in Figure 4 (top). Undoped PEDOT (-0.60 V vs SCE) has a  $\pi$ - $\pi^*$  absorption maximum at 1.97 eV and a bandgap of 1.64 eV. It is seen that some phonon sidebands appear as shoulders which points to a rather regular structure. Just as is the case for the solid

**Table 5. Oxidation Potentials,  $E_{ox}$ , Bandgaps,  $E_g$ , and NIR Maxima,  $E_1$ ,  $E_2$  (at Low Doping Levels), and  $E_3$  (at High Doping Levels)**

polymer		$E_{ox}$ (V vs SCE)	$E_{max}$ (eV)	$E_g$ (eV)	$E_1$ (eV)	$E_2$ (eV)	$E_3$ (eV)	$E_2/E_g$
<b>1</b>	film	+0.36	1.88	1.52		1.10	0.81	
	solid solution		2.00	1.67	0.65	1.00	0.88	0.60
<b>2</b>	film	+0.65	2.02	1.56		1.16	0.88	
	solid solution		2.08	1.79	0.68	0.97	0.74	0.54
<b>3</b>	film	+0.57	2.13	1.69		1.02	0.88	
	solid solution		2.12	1.79	0.78	1.00	0.81	0.56
<b>4</b>	film	+0.44	2.06	1.57		1.17	0.93	
	solid solution		2.16	1.65	0.72	1.16	1.22	0.70
PEDOT-C <sub>6</sub>	film	-0.04	1.97	1.80	≤0.6	1.25	≤0.6	0.69
PEDOT	film	-0.13	1.91	1.64	≤0.6	1.35	≤0.6	0.80
PT	film	+0.7	2.61	2.0	0.66	1.55	1.06	0.78
PTV	film	+0.75	2.6	1.9				

PAOTVs, the spectrum shows some absorption features below 1.6 eV, again probably due to some trapped charged defects.

The absorption strength of the main band decreases upon doping, but in contrast to the case of the PAOTVs no shift in energy is observed. At low doping levels two new absorption bands appear (at ≤0.6 and 1.35 eV, respectively). At increased doping levels the low energy band at about 0.6 eV grows steadily, whereas the band at 1.35 eV first increases somewhat but gradually decreases again. At maximum doping level the PEDOT coating is rather transparent in the visible region. The original  $\pi-\pi^*$  absorption band has disappeared completely and the remaining absorption in the visible region, probably due to the tail of the NIR band, is small. Dedoping the PEDOT film leads to a spectrum (labeled -0.6 V\*) that does not differ significantly from that of the original PEDOT. Again, just as in the case of the PAOTVs, the combined oscillator strengths of the NIR absorption bands at maximum doping (0.20 per repeat unit) is larger than that of the decrease in oscillator strength of the original  $\pi-\pi^*$  absorption band of the undoped material (-0.14 per repeat unit).

In an attempt to solubilize PEDOT we also prepared the polymer PEDOT-C<sub>6</sub> in which each ethylene dioxide bridge is provided with an *n*-hexyl group in a regional nonspecific way. However, PEDOT-C<sub>6</sub> was insoluble in all solvents we tried. The absorption spectra of a (PEDOT-C<sub>6</sub>) film, prepared analogously to the PEDOT coating, are shown at various stages of electrochemical doping in Figure 3 (bottom). In this case the phonon side bands are very clear, even in a slightly doped state, indicating increased regularity of the conjugated chains. The absorption maximum in the undoped state is found at 1.91 eV. However, for a fair comparison with PEDOT, where the maximum occurs at the second peak at 1.97 eV, the value 2.07 eV for this peak in PEDOT-C<sub>6</sub> should be taken. The  $\pi-\pi^*$  absorption band in PEDOT-C<sub>6</sub> is shifted toward higher energies as compared with PEDOT, and so is the bandgap (1.80 eV vs 1.64 eV for PEDOT). The behavior upon doping of PEDOT-C<sub>6</sub> is very similar to that of PEDOT. NIR bands grow in the same way and at about the same energies, up to a total oscillator strength of 0.31 per repeat unit, and the original  $\pi-\pi^*$  absorption band of an oscillator strength of 0.24 per repeat unit disappears completely without intermediate energy shifts. Recent results on PEDOT-C<sub>8</sub> and PEDOT-C<sub>14</sub><sup>13</sup> are very similar to our results on PEDOT-C<sub>6</sub>. The conductivities of PEDOT and PEDOT-C<sub>6</sub> were measured on films as

prepared (Table 4). The maximum doping levels both in PEDOT and in PEDOT-C<sub>6</sub> were estimated at  $0.45 \pm 0.1$ . A real determination scattered for the same reason as in the PAOTVs, albeit that the current tails in the latter were more pronounced.

#### 4. Discussion

**4.1. Oxidation Potentials and Bandgaps.** The oxidation potentials and the bandgaps of films of the PAOTVs 1–4 are given in Table 5, together with those of films of PEDOT, PEDOT-C<sub>6</sub>, polythiophene (PT),<sup>14</sup> and poly(thiophene-vinylene) (PTV).<sup>15</sup> The properties of the alkoxy-substituted polymers are very sensitive to the orientation of the oxygen lone pairs with respect to the conjugated  $\pi$ -electron system. Namely, the influence of an alkoxy group on the conjugated system comprises an inductive effect (negative, -I) as well as a mesomeric effect (positive, +M). Maximum overlap between the lone pair orbital of oxygen and the  $\pi$ -orbital of the neighboring carbon atom of the conjugated system is obtained when the O-CH<sub>2</sub> group lies in the plane of the conjugated chain. Then the +M effect is at a maximum and much larger than -I, and the alkoxy group is strongly electron donating. If the O-CH<sub>2</sub> group is rotated out of the plane of the conjugated system, the +M effect decreases and the alkoxy group becomes less donating. In PEDOT the orientation is fixed by the ethylene bridge to be slightly out of the plane. The decrease in oxidation potential of nearly 1 V in going from PT to PEDOT shows that in PEDOT a strong donating effect is present. The oxidation potential of PEDOT-C<sub>6</sub> is larger than that of PEDOT by about 0.1 V, probably due to a small sterical effect of the hexyl chains leading to a distortion of the planarity of the conjugated system. The same effect explains the small difference in the bandgap of these polymers. In even alternate conjugated systems the attachment of an electron-donating group gives, in first order, no change in the bandgap. The HOMO  $\pi$  and the LUMO  $\pi^*$  level are shifted by equal amounts, because the coefficients of the wave functions of both levels are equal.<sup>16</sup> However, in polythiophene the HOMO is confined to the carbon atoms, whereas the LUMO shows appreciable density on the sulfur atom and a smaller density on the carbon atoms.<sup>17</sup> It follows that in PEDOT the  $\pi^*$  level

(14) Kaneto, K.; Kohno, Y.; Yoshino, K. *Mol. Cryst. Liq. Cryst.* **1985**, *118*, 217–220.

(15) Onoda, M.; Iwasa, T.; Kawai, T.; Yoshino, K. *J. Phys. D: Appl. Phys.* **1991**, *24*, 2076–2083.

(16) Griffith, J. *Colour and Constitution of Organic Molecules*; Academic Press: London, 1976; p 93.

(17) Tol. A., personal communication.

(13) Sankaran, B.; Reynolds, J. R. *Polym. Mater. Sci. Eng.* **1995**, *72*, 319–320.

is shifted by a smaller amount than the  $\pi$  level, leading to a smaller bandgap than that of PT.

The oxidation potential of **4** is higher than that of PEDOT-C<sub>6</sub> because of the influence of the connecting vinyl groups that are less electronegative than PEDOT. The increase in the oxidation potential of the PAOTVs in going from **4** through **3** to **2** may be ascribed to increased steric hindrance of the alkoxy substituents, leading to configurations in which the O-CH<sub>2</sub> groups are in the less-donating positions out of the plane of the conjugated system. Surprisingly, the lowest oxidation potential in the PAOTVs, 0.39 V lower than that of PTV, is found for the monoalkoxy-substituted polymer **1**. A similar decrease of 0.43 V was found for poly(3-ethoxythiophenylene-vinylene).<sup>12</sup> Absolute values of the oxidation potentials are difficult to compare due to the uncertainty of the dependence of reference potentials on the solvents used. In the monoalkoxy polymers the absence of steric hindrance makes the optimum position of the O-CH<sub>2</sub> group possible, and the resulting strong donating properties of the single alkoxy group exceeds that of two hindered alkoxy groups in the other PAOTVs. For the same reason as in PEDOT (see preceding paragraph), the LUMO levels are less influenced by the donating alkoxy groups than the HOMO levels are. Indeed the bandgaps of all four PAOTVs are smaller than that of PTV. In the PAOTV films **1**, **4**, and **3** the increase of the bandgap is approximately proportional to the increase in oxidation potential, but in **2** a deviation of this expected behavior is found.

The bandgaps of the solid PAOTVs are smaller than those in solution. A difference of about 0.1 eV is generally found for conjugated polymers and is ascribed to a tendency toward more planar structures in the solid and, possibly, to some overlapping of the  $\pi$  wave functions of different molecules. A somewhat larger influence of solidification on the bandgaps of the monododecylalkoxy PAOTV **1** (0.15 eV) and bisdodecylalkoxy PAOTV **2** (0.23 eV) may be due to the presence of rather well-ordered semicrystalline dodecyl regions, which imposes more order in the stacking of the conjugated chains as well.

**4.2. Vis-NIR Absorption Spectra of Doped Polymers.** At first glance the changes in the vis-NIR absorption spectra with doping are similar for all polymers measured. At low doping levels the intensity of the regular  $\pi$ - $\pi^*$  absorption band in the visible region decreases and two new bands appear in the NIR. The generally accepted explanation of this behavior is that doping extracts levels from the valence and conduction bands to form a half-filled low-energy and an empty high-energy polaron level in the gap.<sup>18,19</sup> Transitions from the valence band to the half-filled polaron level,  $E_1$ , and from this half-filled level to the empty polaron level,  $E_2$ , have in general high transition moments.<sup>19</sup> In this model the ratio  $E_2/E_g$  is a measure of the degree of localization of the polarons. The values of this ratio in the PAOTVs are lower than in the other polymers considered in Table 5, pointing to a stronger tendency to localization. However, the relation  $E_{\max} \approx 2E_1 + E_2$  implied by the model is not too well satisfied. This makes a detailed application doubtful.

At higher doping levels the NIR bands are replaced by a single band, sometimes showing a small high-energy shoulder. This behavior may be described by a bipolaron model.<sup>18,19</sup> In solid PAOTVs a single NIR band is found at all levels of doping, which would mean that the polaron stage is skipped. The observed increase in oscillator strength of the NIR band(s) formed at maximum doping is, for all polymers, larger than the decrease in oscillator strength of the original  $\pi$ - $\pi^*$  absorption band by a factor of 1.2–1.5. This may point to an increase in planarity in going from undoped to doped chains, because torsion always leads to lower absorption intensities.<sup>20</sup> The position of the NIR bands in heavily doped PEDOT and PEDOT-C<sub>6</sub> is at least 0.2 eV lower than that in the other polymers (see Table 5,  $E_3$ ). A higher value of  $E_3$  in the bipolaron model points to a stronger tendency to localization of the charge carriers.

The spectra of PEDOT and PEDOT-C<sub>6</sub> exhibit another striking difference with those of the other polymers. In the spectra of the PAOTVs (in fact of most conjugated polymers known today) both the  $\pi$ - $\pi^*$  absorption band and the NIR bands shift markedly upon increase of doping level, whereas in the case of the PEDOTs the bands only change in intensity but do not shift in energy. It has been proposed that the shift of the  $\pi$ - $\pi^*$  absorption band toward higher energies upon doping reflects the distribution of conjugation lengths in the polymer, chains with the longer conjugation lengths being doped first.<sup>21</sup> A uniform or at least long conjugation length in PEDOT would then be needed to explain the absence of a shift in these cases, which property is by no means obvious in view of the preparation method. Another explanation ascribes the shifts to an increase in bandgap as a consequence of taking out levels, randomly distributed in space, from the top of the valence band and of the bottom of the conduction band to form the polaron levels. The experimental fact that such a shift does not occur in PEDOT, then, would point to a different doping behavior, viz. undoped chains on one hand and chains doped to their full capacitance on the other hand. Possibly the polarons and their supporting counterions form a kind of lattice in PEDOT that is energetically more favorable than separated polarons. This regular way of doping may be the origin of the high conductivity of PEDOT. The fact that no clear isosbestic points are seen in Figure 3, then, would point to a not completely ideal behavior of the whole sample.

In heavily doped samples of three conjugated polymers, viz. PEDOT, polyacetylene, and PANI, conductivities in the range 300–500 S/cm can be measured routinely, exceeding the values found in other heavily doped conjugated polymers by at least a factor of 3. Similar high conductivities were further only found for iodine-doped regioregular poly(3-(2,5,8-trioxanonyl)thiophene).<sup>22,23</sup> For this polymer, however, spectral data have not been published. Such a high and (near-) metallic level of conductivity implies a finite IR absorp-

(18) Furukawa, Y. *Synth. Met.* **1995**, *69*, 629–632.

(19) Fesser, K.; Bishop, A. R.; Campbell, D. K. *Phys. Rev. B* **1983**, *27*, 4804–4816.

(20) Griffith, J. *Colour and Constitution of Organic Molecules*; Academic Press: London, 1976; p 105.

(21) Visy, C.; Lukkari, J.; Kankare, J. *J. Electroanal. Chem.* **1991**, *319*, 85–100.

(22) McCullough, R. D.; Williams, S. P.; Tristram-Nagle, S.; Jayaraman, M.; Ewbank, P. C.; Miller, L. *Synth. Met.* **1995**, *69*, 279–282.

(23) McCullough, R. D.; Williams, S. P. *J. Am. Chem. Soc.* **1993**, *115*, 11608–11609.

**Table 6. Bandgaps of Undoped Polymers,  $E_g$ , and NIR Maxima,  $E_3$ , Absorption Coefficients at 2.1 eV,  $\epsilon$ , and Conductivities,  $\sigma$ , in the Heavily Doped State**

polymer	$E_g$ (eV)	$E_3$ (eV)	$10^4\epsilon$ (cm <sup>-1</sup> )	$\sigma$ (S/cm)
<b>1</b>	1.52	0.81	2.6	2
<b>2</b>	1.56	0.88	3.8	0.1
<b>3</b>	1.69	0.88	3.3	0.2
<b>4</b>	1.57	0.93	3.4	0.35
PEDOT	1.64	≤0.6	1.4	400
PEDOT-C <sub>6</sub>	1.80	≤0.6	0.7	40
PT	1.98	1.06	8.2 <sup>a</sup>	20
PTV	1.9	1.2 (1.5 sh)	1.3	
PANI		0.65	0.9	300
PITN	1.0	0.75 (1.15 sh)		50

<sup>a</sup> At 2.9 eV.

tion down to 0 eV, which is compatible with the low-energy NIR peaks found in those three polymers. The conductivities that can be obtained in PANI are very strongly dependent on the solvent and dopant used.<sup>24,25</sup> In good solvents isosbestic points have been claimed and interpreted as a two-phase behavior of fully doped and completely undoped chains.<sup>26</sup> We have verified that in the best-known system, PANI/*m*-cresol/camphorsulfonic acid, indeed no shifts in the absorption peaks are found when the doping concentration is varied. In polyacetylene the spectra during the doping process are changing in both intensity and position. The final doping in going from the semiconductive into the metallic regime is accompanied by a shift in the NIR absorption band from 0.7 to below 0.6 eV.<sup>27,28</sup> Possibly doping starts randomly in polyacetylene, but at very high concentrations a more regular lattice of charge carriers and counterions is formed, leading to high conductivities.

**4.3. Transparency and Conductivity.** From the data summarized in Table 6 it is immediately clear that the newly synthesized PAOTVs have not brought the wanted improved materials for transparent conductive coatings. Namely, while the remaining absorption in the visible region is even somewhat larger than that of PEDOT, the conductivities obtained are 2–3 orders of magnitude lower. The low degree of polymerization can explain 1 order of magnitude only. The stronger localization of the charge carriers in these PAOTVs (see above) and a lower maximum doping level may be related to the remaining differences. Although the insertion of a vinylene bridge indeed leads to a somewhat lower bandgap, the NIR peak in heavily doped PAOTVs is at about 0.2 eV higher energy. Also the attempt to make PEDOT soluble by adding a hexyl group to the ethylenedioxiide bridge (PEDOT-C<sub>6</sub>) gives a polymer that is still insoluble, and the other properties have, at least, not improved.

For comparison we have also included data of polyisothionaphthene (PITN).<sup>29,30</sup> The changes in the absorption spectra for this compound point to random doping,

and the measured conductivity is indeed of the order of that of PT. However, this material has an extremely small bandgap, which explains the position of the NIR maximum at doping, leading to a rather transparent material. The remaining color is yellow due to absorption in the high energy part of the visible region caused by tails of UV absorptions. The bluish color of PEDOT is caused by a tail of the NIR absorption, the green color of PANI to tails at both sides of the visible region.

Materials of choice for transparent conductive coatings are still PEDOT and PANI, combining low absorption, high conductivity, and high stability. Polyacetylene is too unstable in the doped state to be useful, and both the conductivity and the stability of PITN are rather low. What, then, makes PEDOT and PANI so special? In this study we have found that in both PEDOT and PANI the doping process differs from that in the other polymers, involving no shifts in absorption peaks and leading to low-lying NIR absorption bands at less than 0.6 eV. Transparency is due to the as-yet not understood low-energy of this NIR band in the highly doped state. The high conductivities observed are probably connected with a more regular structure of the doped polymers. The low oxidation potentials (<0 V vs SCE) contribute to the stability of the p-type doped state.

## 5. Conclusions

The “Stille” coupling reaction has been used to synthesize four different alkoxy-substituted polythiophene–vinylenes (PAOTVs). The degree of polymerization varies between 7 and 50 monomer units depending on the oligomer in question. Instability of the dibromoalkoxy-substituted thiophene starting compounds prevented higher degrees of polymerization.

The introduction of a vinylene spacer between monomer units of PEDOT lowers the bandgap, but as at maximum doping the NIR absorption bands are blue-shifted by about 0.2–0.3 eV, the transmittance is lower than that of PEDOT. Moreover, the conductivity is 3 orders of magnitude lower. The other three PAOTVs have similar properties.

The doping behavior as a function of the doping level of PEDOT and of PANI is significantly different from those of polythiophene and the PAOTVs. In the case of PEDOT and PANI the maxima of the NIR absorption bands and the maximum of the  $\pi$ – $\pi^*$  absorption band do not shift during doping. For all other polymers one finds shifts in the energies of all bands. At full doping the NIR bands in PEDOT and in PANI are at about 0.5 eV, much lower than in the PAOTVs.

Materials of choice for transparent conductive coatings are still PEDOT and PANI, combining low absorption, high conductivity, and high stability.

**Acknowledgment.** We thank our colleagues at the Philips Research Laboratory: M. Simenon (advice electrochemical experiments), W. Keur and H. van Hal (synthesis tris(paratoluenesulfonate)Iron(III) hexahydrate), W. Rutten (GPC measurements), P. Kruseman, M. van der Straaten, and A. de Jong (elemental analysis), and J. M. Toussaint (University of Mons, Belgium), D. de Leeuw, and A. Tol for critical discussions.

CM9504551

- (24) Cao, Y.; Qui, J.; Smith, P. *Synth. Met.* **1995**, *69*, 187–190.  
 (25) Cao, Y.; Smith, P. *Synth. Met.* **1995**, *69*, 191–192.  
 (26) Masters, J. G.; Sun, Y.; MacDiarmid, A. G.; Epstein, A. J. *Synth. Met.* **1991**, *41–43*, 715–718.  
 (27) Fincher, C.; Ozaki, M.; Tanaka, M.; Peebles, D.; Lauchlan, L.; Heeger, A. *Phys. Rev. B* **1982**, *20*, 1589–1602.  
 (28) Feldblum, A.; Kaufman, J. H.; Etemad, S.; Heeger, A. J. *Phys. Rev. B* **1982**, *26*, 815–826.  
 (29) Kobayashi, M.; Colaneri, N.; Boysel, M.; Wudl, F.; Heeger, A. J. *J. Chem. Phys.* **1985**, *82*, 5717–5723.  
 (30) Colaneri, N.; Kobayashi, M.; Heeger, A. J.; Wudl, F. *Synth. Met.* **1986**, *14*, 45–52.